Guidance-Based Path Following for Autonomous Underwater Vehicles

Morten Breivik*,[1]
*Centre for Ships and Ocean Structures (CESOS)
Norwegian University of Science and Technology (NTNU)
NO-7491 Trondheim, Norway
E-mail: morten.breivik@ieee.org

Thor I. Fossen*,†
†Department of Engineering Cybernetics (ITK)
Norwegian University of Science and Technology (NTNU)
NO-7491 Trondheim, Norway
E-mail: fossen@ieee.org

***Abstract*— This paper addresses the problem of path following for autonomous underwater vehicles (AUVs) by utilizing a novel guidance-based approach. Termed guidance-based path following, the proposed approach is equally applicable for sea, land and air vehicles. This relates to the fact that the core guidance laws are developed at an ideal, dynamics-independent level, entailing generally valid laws uninfluenced by the particularities of any specific dynamics case. The laws can subsequently be tailored to specific target systems like AUVs. A nonlinear, model-based velocity and attitude controller, which depends fully on the guidance system reference signals in order to fulfill the guidance-based path following task objectives, is proposed for the purpose of controlling both fully actuated and underactuated AUVs. The resulting guidance and control scheme renders all regular paths feasible, and simulation results successfully demonstrate its capability.**

I. Introduction

The number of autonomous underwater vehicles (AUVs) roaming the seas of the world is rapidly increasing, mainly due to tasks originating from various commercial, military and scientific needs. In this context, the ability for the AUVs to maneuver accurately and safely both in space and time is important. Traditionally, the concept of trajectory tracking (TT) has been invoked when faced with the problem of maneuvering AUVs. However, the TT approach inherently mixes the space and time assignments into one single assignment, demanding that the AUVs are located at a specific point in space at a specific, pre-assigned instant in time. Hence, TT represents in effect a feedforward, open loop type of solution at the path-vehicle interaction level. Its assignments have to be manually reparametrized if something should occur that would render the AUVs incapable of satisfying the initial task objectives. Therefore, it seems that such an approach does not offer the robustness properties necessary for the problem at hand. However, the concept of path following (PF), which emphasizes spatial localization as a primary task objective, and considers the dynamic aspect as a secondary task objective, sacrificable if necessary, represents a more flexible and robust alternative than the TT scheme. Consequently, this paper considers the PF scheme as a framework in which to develop a guidance and control methodology for accurate and safe maneuvering of AUVs in the ocean space.

[1]This work was supported by the Research Council of Norway through the Centre for Ships and Ocean Structures at NTNU.

A. Previous Work

A lot of the research reported on control of AUVs consider only the simplified case of planar motion, see e.g. [1], [2], and [3]. Some research also consider decoupled spatial designs by separating the inherently coupled spatial case into two decoupled planar cases by considering non-interacting horizontal and vertical modes separately, see e.g. the work in [4] for slender-body AUVs. Such an approach can be characterized as a transition between a simplified planar consideration and a full spatial consideration. Coupled spatial considerations can be found in e.g. [5], [6], and [7]. However, in [5] the AUV cannot be located at the center of the sphere of osculation due to the kinematic singularity originating from the choice of stating the path following problem in the Serret-Frenet path frame. Also, the approaches in [6] and [7] involve inherent singularities due to the way in which the control problem is stated and solved. Note that these singularities are not kinematic representational singularities (which for instance can originate from using Euler angles to represent the AUV attitude), but methodologically inherent singularities undesirable from both a theoretical and practical point-of-view.

B. Main Contribution

This paper presents a guidance-based path following scheme for AUVs operating in a 3D ocean space. The consideration is spatially fully coupled, and the scheme renders geometric convergence to all regular paths feasible. It relies on key ideal guidance laws which are equally applicable to aircraft and spacecraft as they are to watercraft. The approach depends on a nonlinear, model-based velocity and attitude controller, and a key feature of the scheme is that it ensures path following for both fully actuated and underactuated AUVs. The paper contains a lucid exposition of the proposed guidance and control methodology, which is physically intuitive.

II. Problem Statement

The primary objective in guidance-based path following is to ensure that a vehicle converges to and follows a desired geometric path, without any temporal requirements. The secondary objective is to ensure that the vehicle complies with a desired dynamic behaviour. By using the convenient task classification scheme in [8], the guidance-based path following problem can thus be expressed by the following two task objectives:

Geometric Task: Make the position of the vehicle converge to and follow a desired geometric path.

Dynamic Task: Make the speed of the vehicle converge to and track a desired speed assignment.

When both task objectives for some reason cannot be met simultaneously, the geometric one has precedence over the dynamic one.

III. Ideal Guidance Concept

The content in this section is taken from [9], where the guidance laws required to solve the spatial guidance-based path following problem in question are originally developed. We will consistently employ the notion of an *ideal particle*, which is to be interpreted as a spatial position variable without dynamics (i.e. it can instantly attain any assigned motion behaviour) free to move anywhere in 3D space. We will also utilize the notion of a *path particle*, which is to be interpreted as a spatial position variable restricted to move along the geometric path it is associated with.

A. Assumptions

The following assumptions are made:

- **A.1** The desired geometric path is regularly parametrized.
- **A.2** The speed of the ideal particle is lower-bounded.
- **A.3** The guidance variables are positive and upper-bounded.

B. Ideal Guidance Laws

Denote the inertial position and velocity vectors of the ideal particle by $\mathbf{p} = [x, y, z]^\top \in \mathbb{R}^3$ and $\dot{\mathbf{p}} = [\dot{x}, \dot{y}, \dot{z}]^\top \in \mathbb{R}^3$, respectively. Denote the size of the velocity vector by $U = |\dot{\mathbf{p}}|_2 = (\dot{\mathbf{p}}^\top \dot{\mathbf{p}})^{\frac{1}{2}}$ (the speed), and let the orientation be characterized by the two angular variables:

$$\chi = \arctan\left(\frac{\dot{y}}{\dot{x}}\right), \tag{1}$$

which is denoted the azimuth angle, and:

$$\upsilon = \arctan\left(\frac{-\dot{z}}{\sqrt{\dot{x}^2 + \dot{y}^2}}\right), \tag{2}$$

denoted the elevation angle. Since it is assumed that for an ideal particle U, χ and υ can attain any desirable value instantaneously, rewrite them as U_d, χ_d and υ_d.

Consider a geometric path continuously parametrized by a scalar variable $\pi \in \mathbb{R}$, and denote the inertial position of its path particle as $\mathbf{p}_\mathrm{p}(\pi) \in \mathbb{R}^3$. Consequently, the geometric path can be expressed by the set:

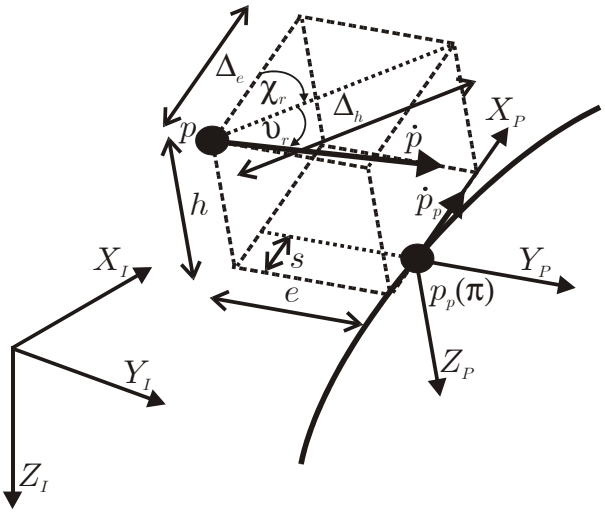

Fig. 1. The geometric relationship between all the relevant parameters and variables utilized in the proposed guidance-based path following scheme in 3D, $\mu = 1$.

$$\mathcal{P} = \left\{\mathbf{p} \in \mathbb{R}^3 \mid \mathbf{p} = \mathbf{p}_\mathrm{p}(\pi)\ \forall \pi \in \mathbb{R}\right\}, \tag{3}$$

where $\mathcal{P} \subset \mathbb{R}^3$.

For a given π, define a local reference frame at $\mathbf{p}_\mathrm{p}(\pi)$ and name it the PATH frame (**P**). To arrive at **P**, we need to perform two consecutive elementary rotations (when using the concept of Euler angles). The first is to positively rotate the INERTIAL frame (**I**) an angle:

$$\chi_\mathrm{p}(\pi) = \arctan\left(\frac{y'_\mathrm{p}(\pi)}{x'_\mathrm{p}(\pi)}\right) \tag{4}$$

about its z-axis, where the notation $x'_\mathrm{p}(\pi) = \frac{\mathrm{d}x_\mathrm{p}}{\mathrm{d}\pi}(\pi)$ has been utilized. This rotation can be represented by the rotation matrix:

$$\mathbf{R}_{\mathrm{p,z}}(\chi_\mathrm{p}) = \begin{bmatrix} \cos\chi_\mathrm{p} & -\sin\chi_\mathrm{p} & 0 \\ \sin\chi_\mathrm{p} & \cos\chi_\mathrm{p} & 0 \\ 0 & 0 & 1 \end{bmatrix}, \tag{5}$$

where $\mathbf{R}_{\mathrm{p,z}} \in SO(3)$. The second rotation is performed by positively rotating the resulting intermediate frame an angle:

$$\upsilon_\mathrm{p}(\pi) = \arctan\left(\frac{-z'_\mathrm{p}(\pi)}{\sqrt{x'_\mathrm{p}(\pi)^2 + y'_\mathrm{p}(\pi)^2}}\right) \tag{6}$$

about its y-axis. This rotation can be represented by the rotation matrix:

$$\mathbf{R}_{\mathrm{p,y}}(\upsilon_\mathrm{p}) = \begin{bmatrix} \cos\upsilon_\mathrm{p} & 0 & \sin\upsilon_\mathrm{p} \\ 0 & 1 & 0 \\ -\sin\upsilon_\mathrm{p} & 0 & \cos\upsilon_\mathrm{p} \end{bmatrix}, \tag{7}$$

where $\mathbf{R}_{\mathrm{p,y}} \in SO(3)$. Hence, the full rotation can be represented by the rotation matrix:

$$\mathbf{R}_{\mathrm{p}} = \mathbf{R}_{\mathrm{p,z}}(\chi_{\mathrm{p}})\mathbf{R}_{\mathrm{p,y}}(\upsilon_{\mathrm{p}}), \tag{8}$$

where $\mathbf{R}_{\mathrm{p}} \in SO(3)$. Consequently, the error vector between $\mathbf{p}$ and $\mathbf{p}_{\mathrm{p}}(\pi)$ expressed in $\mathbf{P}$ is given by:

$$\boldsymbol{\varepsilon} = \mathbf{R}_{\mathrm{p}}^{\top}(\mathbf{p} - \mathbf{p}_{\mathrm{p}}(\pi)), \tag{9}$$

where $\boldsymbol{\varepsilon} = [s, e, h]^{\top} \in \mathbb{R}^3$ consists of the *along-track error* s, the *cross-track error* e, and the *vertical-track error* h; see Figure 1. The along-track error represents the distance from $\mathbf{p}_{\mathrm{p}}(\pi)$ to $\mathbf{p}$ along the x-axis of the PATH frame, the cross-track error represents the distance along the y-axis, while the vertical-track error represents the distance along the z-axis. Also, recognize the notions of the *horizontal-track error* $\sqrt{s^2 + e^2}$, the *generalized cross-track error* $\sqrt{e^2 + h^2}$, and the *off-track error* $\sqrt{s^2 + e^2 + h^2}$.

By differentiating $\boldsymbol{\varepsilon}$ with respect to time, we obtain:

$$\dot{\boldsymbol{\varepsilon}} = \dot{\mathbf{R}}_{\mathrm{p}}^{\top}(\mathbf{p} - \mathbf{p}_{\mathrm{p}}) + \mathbf{R}_{\mathrm{p}}^{\top}(\dot{\mathbf{p}} - \dot{\mathbf{p}}_{\mathrm{p}}), \tag{10}$$

where:

$$\dot{\mathbf{R}}_{\mathrm{p}} = \mathbf{R}_{\mathrm{p}}\mathbf{S}_{\mathrm{p}} \tag{11}$$

with:

$$\mathbf{S}_{\mathrm{p}} = \begin{bmatrix} 0 & -\dot{\chi}_{\mathrm{p}}\cos\upsilon_{\mathrm{p}} & \dot{\upsilon}_{\mathrm{p}} \\ \dot{\chi}_{\mathrm{p}}\cos\upsilon_{\mathrm{p}} & 0 & \dot{\chi}_{\mathrm{p}}\sin\upsilon_{\mathrm{p}} \\ -\dot{\upsilon}_{\mathrm{p}} & -\dot{\chi}_{\mathrm{p}}\sin\upsilon_{\mathrm{p}} & 0 \end{bmatrix}, \tag{12}$$

which is skew-symmetric; $\mathbf{S}_{\mathrm{p}} = -\mathbf{S}_{\mathrm{p}}^{\top}$. We also have that:

$$\dot{\mathbf{p}} = \dot{\mathbf{p}}_{\mathrm{dv}} = \mathbf{R}_{\mathrm{dv}}\mathbf{v}_{\mathrm{dv}}, \tag{13}$$

where $\mathbf{R}_{\mathrm{dv}} \in SO(3)$ represents a rotation matrix from the INERTIAL frame to a frame attached to the ideal particle with its x-axis along the velocity vector of the particle. Let this frame be called the DESIRED VELOCITY frame (**DV**). Hence, the vector $\mathbf{v}_{\mathrm{dv}} = [U_{\mathrm{d}}, 0, 0]^{\top} \in \mathbb{R}^3$ represents the ideal particle velocity with respect to **I**, represented in **DV**. The rotation matrix $\mathbf{R}_{\mathrm{dv}}$ is selected to be defined by:

$$\mathbf{R}_{\mathrm{dv}} = \mathbf{R}_{\mathrm{p}}\mathbf{R}_{\mathrm{r}}, \tag{14}$$

where:

$$\mathbf{R}_{\mathrm{r}} = \mathbf{R}_{\mathrm{r,z}}(\chi_{\mathrm{r}})\mathbf{R}_{\mathrm{r,y}}(\upsilon_{\mathrm{r}}) \tag{15}$$

with $\mathbf{R}_{\mathrm{r}}$, $\mathbf{R}_{\mathrm{r,z}}$, and $\mathbf{R}_{\mathrm{r,y}}$ all elements of $SO(3)$. This way of defining $\mathbf{R}_{\mathrm{dv}}$ entails that the **DV** frame is obtained by first performing an initial rotation represented by $\mathbf{R}_{\mathrm{p}}$, resulting in an intermediate frame parallel to the **P** frame, before a relative rotation represented by $\mathbf{R}_{\mathrm{r}}$ is performed to arrive in **DV**. Obviously, $\mathbf{R}_{\mathrm{r}}$ (i.e. the angular variables χ_{r} and υ_{r}) must be designed to ensure that the generalized cross-track error approaches zero (while $\mathbf{R}_{\mathrm{r}}$ approaches **I**), thus solving the geometric task of the guidance-based path following problem.

Continuing to elaborate on (10), we also have that:

$$\dot{\mathbf{p}}_{\mathrm{p}} = \mathbf{R}_{\mathrm{p}}\mathbf{v}_{\mathrm{p}}, \tag{16}$$

where $\mathbf{v}_{\mathrm{p}} = [U_{\mathrm{p}}, 0, 0]^{\top} \in \mathbb{R}^3$ represents the path particle velocity with respect to **I**, represented in **P**.

By then expanding (10) in light of the recent discussion, we get:

$$\begin{aligned} \dot{\boldsymbol{\varepsilon}} &= (\mathbf{R}_{\mathrm{p}}\mathbf{S}_{\mathrm{p}})^{\top}(\mathbf{p} - \mathbf{p}_{\mathrm{p}}) + \mathbf{R}_{\mathrm{p}}^{\top}(\mathbf{R}_{\mathrm{dv}}\mathbf{v}_{\mathrm{dv}} - \mathbf{R}_{\mathrm{p}}\mathbf{v}_{\mathrm{p}}) \\ &= \mathbf{S}_{\mathrm{p}}^{\top}\boldsymbol{\varepsilon} + \mathbf{R}_{\mathrm{r}}\mathbf{v}_{\mathrm{dv}} - \mathbf{v}_{\mathrm{p}}. \end{aligned} \tag{17}$$

Now define the positive definite and radially unbounded Control Lyapunov Function (CLF):

$$V_{\boldsymbol{\varepsilon}} = \frac{1}{2}\boldsymbol{\varepsilon}^{\top}\boldsymbol{\varepsilon} = \frac{1}{2}(s^2 + e^2 + h^2), \tag{18}$$

and differentiate it with respect to time along the trajectories of $\boldsymbol{\varepsilon}$ to obtain:

$$\begin{aligned} \dot{V}_{\boldsymbol{\varepsilon}} &= \boldsymbol{\varepsilon}^{\top}\dot{\boldsymbol{\varepsilon}} \\ &= \boldsymbol{\varepsilon}^{\top}\left(\mathbf{S}_{\mathrm{p}}^{\top}\boldsymbol{\varepsilon} + \mathbf{R}_{\mathrm{r}}\mathbf{v}_{\mathrm{dv}} - \mathbf{v}_{\mathrm{p}}\right) \\ &= \boldsymbol{\varepsilon}^{\top}\left(\mathbf{R}_{\mathrm{r}}\mathbf{v}_{\mathrm{dv}} - \mathbf{v}_{\mathrm{p}}\right) \end{aligned} \tag{19}$$

since the skew-symmetry of $\mathbf{S}_{\mathrm{p}}$ leads to $\boldsymbol{\varepsilon}^{\top}\mathbf{S}_{\mathrm{p}}^{\top}\boldsymbol{\varepsilon} = 0$. By further expansion, we get:

$$\dot{V}_{\boldsymbol{\varepsilon}} = s(U_{\mathrm{d}}\cos\chi_{\mathrm{r}}\cos\upsilon_{\mathrm{r}} - U_{\mathrm{p}}) + eU_{\mathrm{d}}\sin\chi_{\mathrm{r}}\cos\upsilon_{\mathrm{r}} - hU_{\mathrm{d}}\sin\upsilon_{\mathrm{r}}, \tag{20}$$

from where we choose U_{p} as:

$$U_{\mathrm{p}} = U_{\mathrm{d}}\cos\chi_{\mathrm{r}}\cos\upsilon_{\mathrm{r}} + \gamma s, \tag{21}$$

where $\gamma > 0$ becomes a constant gain parameter in the guidance law. Since π is the actual path parametrization variable that we control for guidance purposes, we need to obtain a relationship between π and U_{p} to be able to implement (21). By using the kinematic relationship given by (16), we get that:

$$\dot{\pi} = \frac{U_{\mathrm{d}}\cos\chi_{\mathrm{r}}\cos\upsilon_{\mathrm{r}} + \gamma s}{\sqrt{x_{\mathrm{p}}'^2 + y_{\mathrm{p}}'^2 + z_{\mathrm{p}}'^2}}, \tag{22}$$

which is non-singular for all paths satisfying assumption A.1. This also shows that **P** is not a so-called Serret-Frenet frame, which is defined at the exact projection point of the ideal particle position onto the geometric path. By choosing U_{p} this way, we achieve:

$$\dot{V}_{\boldsymbol{\varepsilon}} = -\gamma s^2 + eU_{\mathrm{d}}\sin\chi_{\mathrm{r}}\cos\upsilon_{\mathrm{r}} - hU_{\mathrm{d}}\sin\upsilon_{\mathrm{r}}. \tag{23}$$

An attractive choice for χ_{r} could be the physically motivated:

$$\chi_{\mathrm{r}}(e) = \arctan\left(-\frac{e}{\triangle_{\mathrm{e}}}\right), \tag{24}$$

where $\triangle_{\mathrm{e}}$ becomes a time-varying guidance variable satisfying A.3, and which is utilized to shape the convergence behaviour towards the xz-plane of **P**. Such a variable is often referred to as a *lookahead distance* in literature dealing with planar path following along straight lines [10], and the physical interpretation can be derived from Figure 1. Note that other sigmoidal shaping functions are also possible candidates for $\chi_{\mathrm{r}}(e)$, for instance the $\tanh$ function.

The choice for υ_{r} could then be:

$$\upsilon_{\mathrm{r}}(h) = \arctan\left(\frac{h}{\triangle_{\mathrm{h}}}\right), \tag{25}$$

where $\triangle_{\mathrm{h}}$ becomes an additional time-varying guidance variable satisfying A.3. It is utilized to shape the convergence behaviour towards the xy-plane of $\mathbf{P}$. Consequently, by utilizing trigonometric relationships from Figure 1, the derivative of the CLF finally becomes:

$$\dot{V}_{\boldsymbol{\varepsilon}} = -\gamma s^2 - U_{\mathrm{d}}\left[\cos\upsilon_{\mathrm{r}}\frac{e^2}{\sqrt{e^2+\triangle_{\mathrm{e}}^2}} + \frac{h^2}{\sqrt{h^2+\triangle_{\mathrm{h}}^2}}\right], \tag{26}$$

which is negative definite under assumptions A.2 and A.3.

Elaborating on these results, we find that the total dynamic system, which consists of the ideal particle and the path particle, can be represented by the states $\boldsymbol{\varepsilon}$ and π. Moreover, the dynamics are non-autonomous since U_{d}, $\triangle_{\mathrm{e}}$, and $\triangle_{\mathrm{h}}$ can be time-varying. However, by reformulating the time dependence through the introduction of an extra state, the augmented system can be made autonomous:

$$\dot{l} = 1,\ l_0 = t_0 \geq 0, \tag{27}$$

see e.g. [11]. Hence, the augmented system can be represented by the state vector $\mathbf{x} = \left[\boldsymbol{\varepsilon}^\top, \pi, l\right]^\top \in \mathbb{R}^3 \times \mathbb{R} \times \mathbb{R}_{\geq 0}$, and with dynamics represented by the time-invariant ordinary differential equation:

$$\dot{\mathbf{x}} = \mathbf{f}(\mathbf{x}). \tag{28}$$

The time variable for the augmented system is denoted t with initial time $t = 0$, such that $l(t) = t + t_0$. The motivation for this reformulation is that it allows us to utilize set stability analysis for time-invariant systems when concluding on whether the task objectives in the problem statement have been met or not. Hence, define the closed, but unbounded set:

$$\mathcal{E} = \left\{\mathbf{x} \in \mathbb{R}^3 \times \mathbb{R} \times \mathbb{R}_{\geq 0} \mid \boldsymbol{\varepsilon} = \mathbf{0}\right\}, \tag{29}$$

which represents the dynamics of the augmented system when the ideal particle has converged to the path particle, i.e. converged to the path. Also, let:

$$|\mathbf{x}|_{\mathcal{E}} = \inf\left\{\mathbf{x} - \mathbf{y} \mid \mathbf{y} \in \mathcal{E}\right\} \tag{30}$$

$$= (\boldsymbol{\varepsilon}^\top\boldsymbol{\varepsilon})^{\frac{1}{2}} \tag{31}$$

represent a function measuring the distance from $\mathbf{x}$ to $\mathcal{E}$, i.e. the off-track error. Making $|\mathbf{x}|_{\mathcal{E}}$ converge to zero is equivalent to solving the geometric task of the guidance-based path following problem, and the following proposition can now be stated:

Proposition 1: The error set $\mathcal{E}$ is rendered uniformly globally asymptotically and locally exponentially stable (UGAS/ULES) under assumptions A.1-A.3 if π is updated by (22), χ_{r} is equal to (24), and υ_{r} is equal to (25).

Proof: Since the set $\mathcal{E}$ is closed, but not bounded, we initially have to make sure that the dynamic system (28) is forward complete [11], i.e. that for each $\mathbf{x}_0$ the solution $\mathbf{x}(t, \mathbf{x}_0)$ is defined on $[0, \infty\rangle$. This entails that the solution cannot escape to infinity in finite time. By definition, l cannot escape in finite time. Also, (18) and (26) shows that neither can $\boldsymbol{\varepsilon}$. Consequently, (22) shows that π cannot escape in finite time under assumptions A.1 and A.2. The system is therefore forward complete. We also know that $\forall \mathbf{x}_0 \in \mathcal{E}$ the solution $\mathbf{x}(t, \mathbf{x}_0) \in \mathcal{E}\ \forall t \geq 0$ because $\boldsymbol{\varepsilon}_0 = \mathbf{0} \Rightarrow \dot{\boldsymbol{\varepsilon}} = \mathbf{0}$. This renders $\mathcal{E}$ forward invariant for (28) since the system is already shown to be forward complete. Now, having established that (28) is forward complete and that $\mathcal{E}$ is forward invariant, and considering the fact that $V_{\boldsymbol{\varepsilon}} = \frac{1}{2}\boldsymbol{\varepsilon}^\top\boldsymbol{\varepsilon} = \frac{1}{2}(|\mathbf{x}|_{\mathcal{E}})^2$, we can derive our stability results by considering the properties of $V_{\boldsymbol{\varepsilon}}$, see e.g. [8]. Hence, we conclude by standard Lyapunov arguments that the error set $\mathcal{E}$ is rendered UGAS. Furthermore, $\dot{V}_{\boldsymbol{\varepsilon}} = -\gamma s^2 - U_{\mathrm{d}}\left[\frac{e^2}{\triangle_{\mathrm{e}}} + \frac{h^2}{\triangle_{\mathrm{h}}}\right] \leq -\gamma s^2 - U_{\mathrm{d,min}}\left[\frac{e^2}{\triangle_{\mathrm{e,max}}} + \frac{h^2}{\triangle_{\mathrm{h,max}}}\right]$ for the error dynamics at $\boldsymbol{\varepsilon} = \mathbf{0}$, which proves ULES. ■

By stabilizing the error set $\mathcal{E}$, we have achieved the geometric task. The dynamic task is fulfilled by assigning a desired speed U_{d} which satisfies assumption A.2. In total, we have now solved the ideal spatial guidance-based path following problem.

Since $\triangle_{\mathrm{h}}$ can be expressed as:

$$\triangle_{\mathrm{h}} = \mu\sqrt{e^2 + \triangle_{\mathrm{e}}^2}, \tag{32}$$

where $\mu > 0$, we can rewrite (26) as:

$$\dot{V}_{\boldsymbol{\varepsilon}} = -\gamma s^2 - U_{\mathrm{d}}\left[\frac{\mu e^2 + h^2}{\sqrt{\mu^2(e^2+\triangle_{\mathrm{e}}^2) + h^2}}\right] \tag{33}$$

because:

$$\cos\upsilon_{\mathrm{r}} = \frac{\mu\sqrt{e^2+\triangle_{\mathrm{e}}^2}}{\sqrt{\mu^2(e^2+\triangle_{\mathrm{e}}^2) + h^2}} \tag{34}$$

when expressing $\triangle_{\mathrm{h}}$ as in (32). By choosing the desired speed of the ideal particle as:

$$U_{\mathrm{d}} = \kappa\sqrt{\mu^2(e^2+\triangle_{\mathrm{e}}^2) + h^2}, \tag{35}$$

where $\kappa > 0$ is a constant gain parameter, we obtain:

$$\dot{V}_{\boldsymbol{\varepsilon}} = -\gamma s^2 - \mu\kappa e^2 - \kappa h^2, \tag{36}$$

which results in the following proposition:

Proposition 2: The error set $\mathcal{E}$ is rendered uniformly globally exponentially stable (UGES) under assumptions A.1 and A.3 if π is updated by (22), χ_{r} is equal to (24), υ_{r} is equal to (25), and U_{d} satisfies (35).

Proof: The first part of the proof is identical to that of Proposition 1. Hence, we conclude by standard Lyapunov arguments that the error set $\mathcal{E}$ is rendered UGES. ■

Although very powerful, this result is clearly not achievable by physical systems since these exhibit natural limitations on their maximum attainable speed. In this regard, Proposition 1 states the best possible stability property a spatial physical system like an autonomous underwater vehicle can hold.

After having obtained the guidance laws of this section by defining and elaborating on an $\mathbf{R}_{\mathrm{dv}}$ which is constructed by four elementary rotations, and partially defined by $\mathbf{R}_{\mathrm{p}}$, we would now like to define an $\mathbf{R}_{\mathrm{dv}}$ which is constructed by only two elementary rotations. This is interesting from a control perspective, especially if we choose not to operate directly in the configuration space. Hence, consider an $\mathbf{R}_{\mathrm{dv}}$ defined by a positive rotation about the z-axis of $\mathbf{I}$ by a desired azimuth angle χ_{d}, followed by a positive rotation about the y-axis of the resulting intermediate frame by a desired elevation angle υ_{d}:

$$\mathbf{R}_{\mathrm{dv}} = \mathbf{R}_{\mathrm{dv,z}}(\chi_{\mathrm{d}})\mathbf{R}_{\mathrm{dv,y}}(\upsilon_{\mathrm{d}}), \tag{37}$$

where $\mathbf{R}_{\mathrm{dv,z}}$ and $\mathbf{R}_{\mathrm{dv,y}}$ both are elements of $SO(3)$. Obviously, the rotations represented by (14) and (37) are not equivalent, i.e. the y- and z-axes of the two resulting frames are not aligned. However, the rotations map the velocity vector $\mathbf{v}_{\mathrm{dv}}$ equivalently to the INERTIAL frame, which is what matters here. Therefore, by equating the first column (which represents a rotation of the x-axis) of (14) with that of (37), we obtain:

$$\chi_{\mathrm{d}} = \arctan\left(\begin{array}{c}\frac{\cos\chi_{\mathrm{p}}\sin\chi_{\mathrm{r}}\cos\upsilon_{\mathrm{r}}+}{-\sin\chi_{\mathrm{p}}\sin\chi_{\mathrm{r}}\cos\upsilon_{\mathrm{r}}+}\cdots \\ \frac{-\sin\upsilon_{\mathrm{p}}\sin\upsilon_{\mathrm{r}}\sin\chi_{\mathrm{p}}+}{-\sin\upsilon_{\mathrm{p}}\sin\upsilon_{\mathrm{r}}\cos\chi_{\mathrm{p}}+}\cdots \\ \frac{\sin\chi_{\mathrm{p}}\cos\chi_{\mathrm{r}}\cos\upsilon_{\mathrm{p}}\cos\upsilon_{\mathrm{r}}}{\cos\chi_{\mathrm{p}}\cos\chi_{\mathrm{r}}\cos\upsilon_{\mathrm{p}}\cos\upsilon_{\mathrm{r}}}\end{array}\right), \tag{38}$$

and

$$\upsilon_{\mathrm{d}} = \arcsin(\sin\upsilon_{\mathrm{p}}\cos\upsilon_{\mathrm{r}}\cos\chi_{\mathrm{r}} + \cos\upsilon_{\mathrm{p}}\sin\upsilon_{\mathrm{r}}), \tag{39}$$

which are the guidance signals that the velocity vector orientation must satisfy in order to ensure geometric path convergence.

IV. AUV Control Concept

This section presents the control concept which ensures guidance-based path following for autonomous underwater vehicles.

A. Equations of Motion

The 6 degrees-of-freedom (DOFs) kinematics of an AUV can be represented by [12]:

$$\dot{\boldsymbol{\eta}} = \mathbf{J}(\Theta)\boldsymbol{\nu}, \tag{40}$$

where $\boldsymbol{\eta} = [x, y, z, \phi, \theta, \psi]^{\top} \in \mathbb{R}^3 \times \mathcal{S}^3$ (earth-fixed position and attitude), $\Theta = [\phi, \theta, \psi]^{\top} \in \mathcal{S}^3$ (3D torus; three angles defined on $[-\pi, \pi]$), and $\boldsymbol{\nu} = [u, v, w, p, q, r]^{\top} \in \mathbb{R}^6$ (vessel-fixed linear and angular velocities). In what follows, we will also utilize the notation $\mathbf{p} = [x, y, z]^{\top}$, $\mathbf{v} = [u, v, w]^{\top}$, and $\boldsymbol{\omega} = [p, q, r]^{\top}$, all elements of $\mathbb{R}^3$.

Additionally:

$$\mathbf{J}(\Theta) = \left[\begin{array}{cc}\mathbf{R}(\Theta) & \mathbf{0}_{3\times3} \\ \mathbf{0}_{3\times3} & \mathbf{T}(\Theta)\end{array}\right], \tag{41}$$

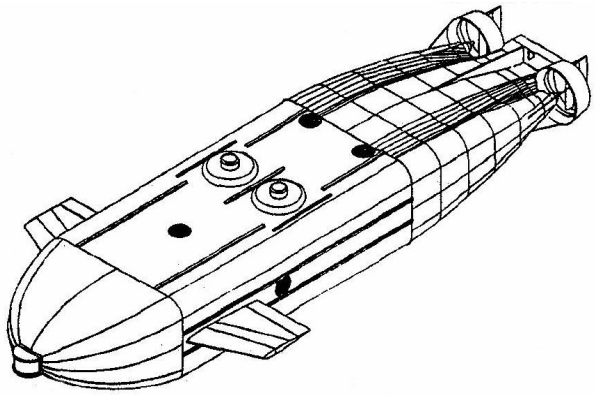

Fig. 2. The MARIUS AUV, a slender-body vehicle primarily designed for flight maneuvers. Courtesy of MARIDAN, http://www.maridan.dk/.

where:

$$\mathbf{R}(\Theta) = \left[\begin{array}{ccc} c\psi c\theta & -s\psi c\phi + c\psi s\theta s\phi & s\psi s\phi + c\psi c\phi s\theta \\ s\psi c\theta & c\psi c\phi + s\phi s\theta s\psi & -c\psi s\phi + s\theta s\psi c\phi \\ -s\theta & c\theta s\phi & c\theta c\phi \end{array}\right] \tag{42}$$

is the rotation matrix from the earth-fixed NED frame (**N**) to the vessel-fixed BODY frame (**B**), parametrized by the three Euler angles in Θ through three consecutive elementary rotations by the zyx-convention. Also:

$$\mathbf{T}(\Theta) = \left[\begin{array}{ccc} 1 & s\phi t\theta & c\phi t\theta \\ 0 & c\phi & -s\phi \\ 0 & s\phi/c\theta & c\phi/c\theta \end{array}\right] \tag{43}$$

relates the vessel-fixed angular velocity vector $\boldsymbol{\omega}$ to $\dot{\Theta}$. For notational brevity, $c\cdot = \cos(\cdot)$, $s\cdot = \sin(\cdot)$, and $t\cdot = \tan(\cdot)$ has been used. At this point, it should be noted that $\mathbf{T}$ is undefined for $\theta = \pm\frac{\pi}{2}$. This is a representational singularity relating to the use of Euler angles for representing the attitude in 3D space (a so-called gimbal lock), and is not kinematically inherent. Such a singularity can be avoided in several ways; by switching between two different Euler angle representations in the vicinity of their singularities, by using a nonsingular four-parameter unit quaternion representation, or by operating directly in the configuration space. However, we will employ the Euler angle zyx-convention in this paper due to the intuition associated with it.

The 6 DOF kinetics of an AUV can be represented by [12]:

$$\mathbf{M}\dot{\boldsymbol{\nu}} + \mathbf{C}(\boldsymbol{\nu})\boldsymbol{\nu} + \mathbf{D}(\boldsymbol{\nu})\boldsymbol{\nu} + \mathbf{g}(\Theta) = \boldsymbol{\tau} + \mathbf{J}(\Theta)^{-1}\mathbf{b}, \tag{44}$$

where $\mathbf{M}$ is the vehicle inertia matrix, $\mathbf{C}(\boldsymbol{\nu})$ is the centrifugal and coriolis matrix, $\mathbf{D}(\boldsymbol{\nu})$ is the hydrodynamic damping matrix, and $\mathbf{g}(\Theta)$ represents hydrostatic forces and moments. The system matrices in (44) are assumed to satisfy the properties $\mathbf{M} = \mathbf{M}^{\top} > 0$, $\mathbf{C} = -\mathbf{C}^{\top}$ and $\mathbf{D} > 0$. Furthermore, $\boldsymbol{\tau}$ represents the vessel-fixed propulsion forces and moments, while $\mathbf{b}$ accounts for the earth-fixed low-frequency environmental forces acting on the vehicle.

B. Control System Design

A nonlinear, model-based velocity and attitude controller is designed by using the backstepping technique. The output-to-be-controlled is redefined from position and attitude to (linear) velocity and attitude. By feeding the controller the appropriate guidance signals, positional convergence is ensured such that the guidance-based path following task objectives are met. This approach resembles the real-life action of a helmsman, who uses vehicle velocity to maneuver. He does not think in terms of directly controlling the position, but in his mind feeds the position error signal back through the velocity assignment, ensuring position control indirectly through direct velocity control. Since such a technique is equally effective for fully actuated and underactuated vehicles, the controller assumes the structure of a velocity and attitude controller.

Start by defining the projection matrix:

$$\mathbf{H} = \begin{bmatrix} \mathbf{0}_{3\times 3} & \mathbf{I}_{3\times 3} \end{bmatrix}, \tag{45}$$

then the error variables:

$$\begin{aligned} \mathbf{z}_1 &= \Theta - \Theta_{\mathrm{d}} && (46)\\ \mathbf{z}_2 &= \boldsymbol{\nu} - \boldsymbol{\alpha}, && (47) \end{aligned}$$

where $\boldsymbol{\alpha} \in \mathbb{R}^6$ is a vector of stabilizing functions to be specified later.

Define the Control Lyapunov Function (CLF):

$$V_1 = \frac{1}{2}\mathbf{z}_1^\top \mathbf{K}_1 \mathbf{z}_1, \tag{48}$$

where $\mathbf{K}_1 = \mathbf{K}_1^\top > 0$. Differentiating V_1 with respect to time along the $\mathbf{z}_1$-dynamics yields:

$$\begin{aligned} \dot{V}_1 &= \mathbf{z}_1^\top \mathbf{K}_1 \dot{\mathbf{z}}_1 \\ &= \mathbf{z}_1^\top \mathbf{K}_1 (\dot{\Theta} - \dot{\Theta}_{\mathrm{d}}) \\ &= \mathbf{z}_1^\top \mathbf{K}_1 (\mathbf{T}\boldsymbol{\omega} - \dot{\Theta}_{\mathrm{d}}), && (49) \end{aligned}$$

since $\dot{\Theta} = \mathbf{T}\boldsymbol{\omega}$. By using (47), we further obtain:

$$\begin{aligned} \dot{V}_1 &= \mathbf{z}_1^\top \mathbf{K}_1 (\mathbf{T}\mathbf{H}(\mathbf{z}_2 + \boldsymbol{\alpha}) - \dot{\Theta}_{\mathrm{d}}) \\ &= \mathbf{z}_1^\top \mathbf{K}_1 \mathbf{T}\mathbf{H}\mathbf{z}_2 + \mathbf{z}_1^\top \mathbf{K}_1 (\mathbf{T}\boldsymbol{\alpha}_{\boldsymbol{\omega}} - \dot{\Theta}_{\mathrm{d}}) && (50) \end{aligned}$$

where $\boldsymbol{\alpha}_{\boldsymbol{\omega}} = \mathbf{H}\boldsymbol{\alpha}$. This motivates the choice of $\boldsymbol{\alpha}_{\boldsymbol{\omega}}$ as:

$$\boldsymbol{\alpha}_{\boldsymbol{\omega}} = \mathbf{T}^{-1}(\dot{\Theta}_{\mathrm{d}} - \mathbf{z}_1), \tag{51}$$

which results in:

$$\dot{V}_1 = -\mathbf{z}_1^\top \mathbf{K}_1 \mathbf{z}_1 + \mathbf{z}_2^\top \mathbf{H}^\top \mathbf{T}^\top \mathbf{K}_1 \mathbf{z}_1. \tag{52}$$

Augment V_1 to obtain:

$$V_2 = V_1 + \frac{1}{2}\mathbf{z}_2^\top \mathbf{M}\mathbf{z}_2 + \frac{1}{2}\tilde{\mathbf{b}}^\top \boldsymbol{\Gamma}^{-1}\tilde{\mathbf{b}}, \tag{53}$$

where $\tilde{\mathbf{b}} \in \mathbb{R}^6$ is an adaptation error defined as $\tilde{\mathbf{b}} = \hat{\mathbf{b}} - \mathbf{b}$ with $\hat{\mathbf{b}}$ being the estimate of $\mathbf{b}$, and by assumption $\dot{\mathbf{b}} = \mathbf{0}$. $\boldsymbol{\Gamma} = \boldsymbol{\Gamma}^\top > 0$ is the adaptation gain matrix.

Differentiating V_2 along the trajectories of $\mathbf{z}_1$, $\mathbf{z}_2$, and $\tilde{\mathbf{b}}$, we obtain:

$$\dot{V}_2 = -\mathbf{z}_1^\top \mathbf{K}_1 \mathbf{z}_1 + \mathbf{z}_2^\top (\mathbf{H}^\top \mathbf{T}^\top \mathbf{K}_1 \mathbf{z}_1 + \mathbf{M}\dot{\mathbf{z}}_2) + \tilde{\mathbf{b}}^\top \boldsymbol{\Gamma}^{-1}\dot{\hat{\mathbf{b}}}, \tag{54}$$

since $\mathbf{M} = \mathbf{M}^\top$ and $\dot{\tilde{\mathbf{b}}} = \dot{\hat{\mathbf{b}}}$. By rewriting $\mathbf{g}(\Theta) = \mathbf{g}$, $\mathbf{C}(\boldsymbol{\nu}) = \mathbf{C}$, and $\mathbf{D}(\boldsymbol{\nu}) = \mathbf{D}$ from (44) for notational brevity, we have that:

$$\begin{aligned} \mathbf{M}\dot{\mathbf{z}}_2 &= \mathbf{M}(\dot{\boldsymbol{\nu}} - \dot{\boldsymbol{\alpha}}) \\ &= \boldsymbol{\tau} + \mathbf{J}^{-1}\mathbf{b} - \mathbf{g} - \mathbf{D}\boldsymbol{\nu} - \mathbf{C}\boldsymbol{\nu} - \mathbf{M}\dot{\boldsymbol{\alpha}}, && (55) \end{aligned}$$

which yields:

$$\begin{aligned} \dot{V}_2 &= -\mathbf{z}_1^\top \mathbf{K}_1 \mathbf{z}_1 + \mathbf{z}_2^\top (\mathbf{H}^\top \mathbf{T}^\top \mathbf{K}_1 \mathbf{z}_1 + \boldsymbol{\tau} + \mathbf{J}^{-1}\mathbf{b} - \mathbf{g}) + \\ &\quad \mathbf{z}_2^\top (-\mathbf{D}\boldsymbol{\nu} - \mathbf{C}\boldsymbol{\nu} - \mathbf{M}\dot{\boldsymbol{\alpha}}) + \tilde{\mathbf{b}}^\top \boldsymbol{\Gamma}^{-1}\dot{\hat{\mathbf{b}}}. && (56) \end{aligned}$$

Utilizing the fact that $\boldsymbol{\nu} = \mathbf{z}_2 + \boldsymbol{\alpha}$ and $\mathbf{b} = \hat{\mathbf{b}} - \tilde{\mathbf{b}}$, we obtain:

$$\begin{aligned} \dot{V}_2 &= -\mathbf{z}_1^\top \mathbf{K}_1 \mathbf{z}_1 - \mathbf{z}_2^\top \mathbf{D}\mathbf{z}_2 - \mathbf{z}_2^\top \mathbf{C}\mathbf{z}_2 + \\ &\quad \mathbf{z}_2^\top (\mathbf{H}^\top \mathbf{T}^\top \mathbf{K}_1 \mathbf{z}_1 + \boldsymbol{\tau} + \mathbf{J}^{-1}\hat{\mathbf{b}} - \mathbf{g}) + && (57)\\ &\quad \mathbf{z}_2^\top (-\mathbf{D}\boldsymbol{\alpha} - \mathbf{C}\boldsymbol{\alpha} - \mathbf{M}\dot{\boldsymbol{\alpha}}) + && (58)\\ &\quad \tilde{\mathbf{b}}^\top \boldsymbol{\Gamma}^{-1}(\dot{\hat{\mathbf{b}}} - \boldsymbol{\Gamma}\mathbf{J}^{-\top}\mathbf{z}_2), && (59) \end{aligned}$$

where $\mathbf{z}_2^\top \mathbf{C}\mathbf{z}_2 = 0$ since $\mathbf{C}$ is skew-symmetric [12]. By assigning:

$$\boldsymbol{\tau} = \mathbf{M}\dot{\boldsymbol{\alpha}} + \mathbf{C}\boldsymbol{\alpha} + \mathbf{D}\boldsymbol{\alpha} + \mathbf{g} - \mathbf{J}^{-1}\hat{\mathbf{b}} - \mathbf{H}^\top \mathbf{T}^\top \mathbf{K}_1 \mathbf{z}_1 - \mathbf{K}_2 \mathbf{z}_2, \tag{60}$$

where $\mathbf{K}_2 = \mathbf{K}_2^\top > 0$, and by choosing:

$$\dot{\hat{\mathbf{b}}} = \boldsymbol{\Gamma}\mathbf{J}^{-\top}\mathbf{z}_2, \tag{61}$$

we finally obtain:

$$\dot{V}_2 = -\mathbf{z}_1^\top \mathbf{K}_1 \mathbf{z}_1 - \mathbf{z}_2^\top (\mathbf{D} + \mathbf{K}_2)\mathbf{z}_2. \tag{62}$$

By a slight abuse of notation, regarding the global nature of the stability in question (which strictly is not satisfied due to the representational singularity of the chosen kinematics at $\theta = \pm\frac{\pi}{2}$), we arrive at the following proposition:

Proposition 3: For smooth reference trajectories $\mathbf{v}_{\mathrm{d}}$, $\dot{\mathbf{v}}_{\mathrm{d}} \in \mathcal{L}_\infty$ and Θ_{d}, $\dot{\Theta}_{\mathrm{d}}$, $\ddot{\Theta}_{\mathrm{d}} \in \mathcal{L}_\infty$, the origin of the error system $\left[\mathbf{z}_1^\top, \mathbf{z}_2^\top, \tilde{\mathbf{b}}^\top\right]^\top$ becomes UGAS/ULES by choosing the control and disturbance adaptation laws as in (60) and (61), respectively.

Proof: [Indication] The proof can be carried out by utilizing Theorem A.5 from [12]. ■

Please note that this velocity and attitude controller in itself achieves nothing unless it is fed the proper reference signals from a guidance system.

V. AUV Guidance Concept

We now look at the design of the reference signals required for guiding a controlled AUV such that it meets the guidance-based path following task objectives, and start out by defining Θ_{d}. Since we rely on the guidance laws from Section III to ensure path following, we will utilize the definition of the desired rotation matrix $\mathbf{R}_{\mathrm{dv}}$ as given in (37) for the purpose, as we have chosen not to operate directly in the configuration space. This means that we want the velocity vector of the AUV to be oriented in 3D space as given by the Euler angles χ_{d} and υ_{d}. However, the actual velocity vector is oriented in 3D space as given by χ and υ from (1) and (2), respectively. These Euler angles define the rotation matrix $\mathbf{R}_{\mathrm{v}} \in SO(3)$, representing a rotation from **N** to the VELOCITY frame (**V**) by:

$$\mathbf{R}_{\mathrm{v}} = \mathbf{R}_{\mathrm{v,z}}(\chi)\mathbf{R}_{\mathrm{v,y}}(\upsilon), \tag{63}$$

while the rotation matrix $\mathbf{R}_{\mathrm{b}} \in SO(3)$, representing a rotation from **N** to **B** have already been defined in (42) by the zyx-convention. Consequently, we define the sideslip angle β by:

$$\beta = \chi - \psi, \tag{64}$$

and the angle-of-attack α by:

$$\alpha = \upsilon - \theta, \tag{65}$$

deviating from the definitions of β and α traditionally found in the hydro- and aerodynamics literature, like [13] and [14]. However, (64) and (65) represents appropriate definitions from a guidance point-of-view, which is of our concern. Consequently, the desired rotation matrix $\mathbf{R}_{\mathrm{db}} \in SO(3)$, representing a rotation from **N** to the DESIRED BODY frame (**DB**) is defined by three consecutive elementary rotations (adhering to the zyx-convention) by:

$$\mathbf{R}_{\mathrm{db}} = \mathbf{R}_{\mathrm{db,z}}(\psi_{\mathrm{d}})\mathbf{R}_{\mathrm{db,y}}(\theta_{\mathrm{d}})\mathbf{R}_{\mathrm{db,x}}(\phi_{\mathrm{d}}) \tag{66}$$

where:

$$\psi_{\mathrm{d}} = \chi_{\mathrm{d}} - \beta \tag{67}$$
$$\theta_{\mathrm{d}} = \upsilon_{\mathrm{d}} - \alpha \tag{68}$$
$$\phi_{\mathrm{d}} = \phi_{\mathrm{d}}, \tag{69}$$

which then constitute Θ_{d}, i.e. $\Theta_{\mathrm{d}} = [\phi_{\mathrm{d}}, \theta_{\mathrm{d}}, \psi_{\mathrm{d}}]^{\top} \in \mathcal{S}^3$. This Θ_{d} applies regardless of the actuator capability of the AUV in question, and together with Θ it defines $\boldsymbol{\alpha}_{\boldsymbol{\omega}}$ through (51).

The control vector of a fully actuated AUV is given by:

$$\boldsymbol{\tau} = [\tau_{\mathrm{X}}, \tau_{\mathrm{Y}}, \tau_{\mathrm{Z}}, \tau_{\mathrm{K}}, \tau_{\mathrm{M}}, \tau_{\mathrm{N}}]^{\top}, \tag{70}$$

which means that the AUV can independently control all DOFs simultaneously, i.e. independently control the linear velocity and the attitude. Hence, while the velocity vector is required to adhere to the guidance laws from Section III in order to achieve path convergence, the attitude can satisfy some auxiliary task objectives. In this context, define the rotation matrix:

$$\mathbf{R}_{\mathrm{gb}} = \mathbf{R}_{\mathrm{gb,z}}(\psi_{\mathrm{g}})\mathbf{R}_{\mathrm{gb,y}}(\theta_{\mathrm{g}})\mathbf{R}_{\mathrm{gb,x}}(\phi_{\mathrm{g}}), \tag{71}$$

representing a rotation from **N** to a GEARED BODY frame (**GB**), $\mathbf{R}_{\mathrm{gb}} \in SO(3)$. The **GB** frame represents the reference attitude that only a fully actuated AUV can attain, and Θ_{g} can be given directly by a human operator or through some high-level guidance system functionality. Note that $\phi_{\mathrm{g}} = \phi_{\mathrm{d}}$. Since we have that:

$$\mathbf{R}_{\mathrm{gb}}\mathbf{v}_{\mathrm{gb}} = \mathbf{R}_{\mathrm{dv}}\mathbf{v}_{\mathrm{dv}}, \tag{72}$$

we get that:

$$\mathbf{v}_{\mathrm{gb}} = \mathbf{R}_{\mathrm{gb}}^{\top}\mathbf{R}_{\mathrm{dv}}\mathbf{v}_{\mathrm{dv}}, \tag{73}$$

which gives us the desired body-fixed linear velocity:

$$\mathbf{v}_{\mathrm{d}} = \mathbf{v}_{\mathrm{gb}}, \tag{74}$$

which also constitutes $\boldsymbol{\alpha}_{\mathbf{v}}$. Finally, higher order derivatives of $\mathbf{v}_{\mathrm{d}}$ and Θ_{d} can be generated by processing them through a reference model which is adjusted to the closed loop AUV dynamics.

The control vector of the most common type of underactuated AUVs in operation is given by:

$$\boldsymbol{\tau} = [\tau_{\mathrm{X}}, 0, 0, 0, \tau_{\mathrm{M}}, \tau_{\mathrm{N}}]^{\top}, \tag{75}$$

which means that only the surge, pitch and yaw DOFs are actuated. In this case, the linear velocity and the attitude of the AUV are inextricably linked together and cannot be controlled independently of each other. This entails that the attitude must be actively used to point the linear velocity vector in the direction suggested by the guidance system in order to achieve path convergence. Equation (60) can still be kept valid by assigning the required expressions to τ_{X}, τ_{M} and τ_{N}, while simultaneously imposing dynamics on the stabilizing functions corresponding to the unactuated DOFs such that (60) is satisfied [15]. An analysis of the resulting $\boldsymbol{\alpha}$-subsystem reveals that the stabilizing functions, and hence also the sway, heave and roll speeds, remain bounded. This is an inherent feature of the ambient water-vehicle system due to the desirable property of hydrodynamic damping.

VI. AUV Guidance and Control Concept

Summing up, the proposed velocity and attitude controller from Section IV relies upon the reference signals supplied by the suggested guidance system from Section V in order to guarantee positional convergence to any regularly parametrized geometric path in 3D space. As long as (60) and (61) are satisfied, the guidance and control concept is equally effective for both fully actuated and underactuated autonomous underwater vehicles. The closed loop behaviour of a guided and controlled AUV naturally depends on the parameters and variables of the guidance and control systems, and can be analyzed for instance in a cascaded setting.

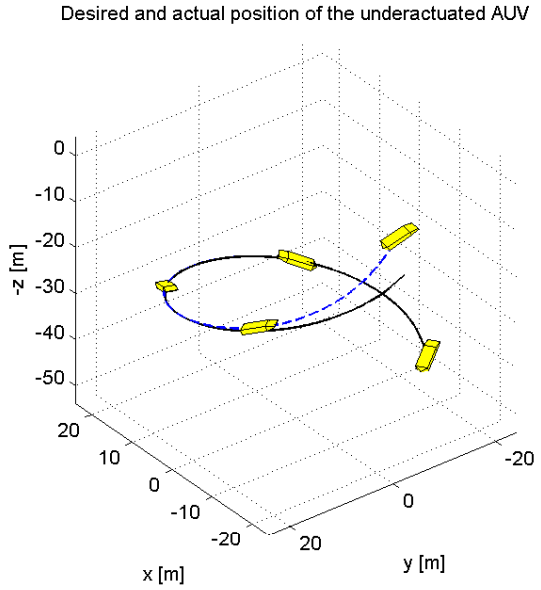

Fig. 3. The underactuated AUV converges naturally to the desired path.

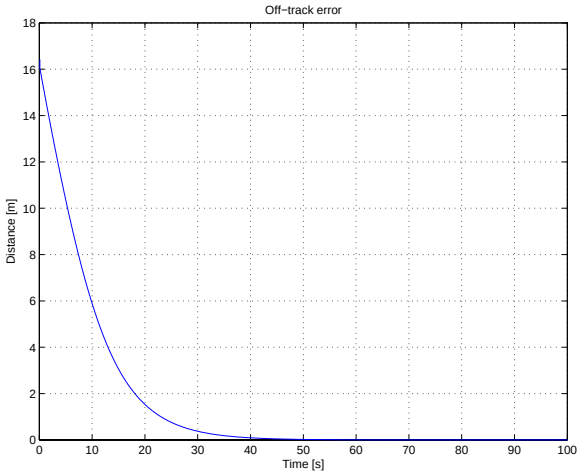

Fig. 4. The off-track error converges to zero.

VII. Case Study: An Underactuated AUV

For the sake of illustration, a simulation is performed with an AUV undertaking a helical flight maneuver, hence representing an underactuated AUV unactuated in the sway, heave, and roll DOFs. The vehicle data is taken from the NPS AUV II, a slender-body AUV with a mass of $m = 5454.54$ kg and a length of $L = 5.3$ m [4]. The AUV is exposed to a constant environmental force during the run.

The initial vehicle states are chosen as $\boldsymbol{\eta}_0 = [-25, 0, 0, 0, 0.17, 0.44]^\top$ (units $[m]$ and $[rad]$), and $\boldsymbol{\nu}_0 = [1.5, 0, 0, 0, 0, 0]^\top$ (units $[m/s]$ and $[rad/s]$), where the initial surge speed is to be kept during the run. The guidance parameter is fixed at $\gamma = 100$, while the guidance variables are chosen by $\triangle_{\mathrm{e}}(t) = U(t)\frac{\triangle_0}{\sqrt{e(t)^2+\triangle_0^2}}$, $\triangle_0 = 2L$, and $\mu = 1$. The controller and adaptation gains are chosen as $\mathbf{K}_1 = \mathbf{K}_2 = 10^3\mathbf{I}$, and $\boldsymbol{\Gamma} = 10^2\mathbf{I}$, respectively.

Figure 3 shows that the AUV converges elegantly to the path while behaving as a weathervane; pointing towards the environmental disturbance. Figure 4 illustrates that the off-track error effectively converges to zero.

VIII. Conclusions

A guidance-based path following approach has been proposed for the purpose of maneuvering AUVs along designated paths in a 3D ocean space. The guidance laws were first developed at a dynamics-independent level, ensuring generally valid laws uninfluenced by any particular dynamics case. Subsequently, these laws were integrated into the guidance system of the specific target system in question to serve as reference signals for a proposed nonlinear, model-based velocity and attitude controller. The resulting guidance and control scheme renders all regular paths feasible for both fully actuated and underactuated AUVs, and simulation results successfully demonstrate the capability of the approach when applied to an underactuated AUV in flight.

References

[1] M. Caccia, G. Bruzzone, and G. Veruggio, "Guidance of unmanned underwater vehicles: Experimental results," in *Proceedings of the ICRA'00, San Francisco, California, USA*, 2000.

[2] K. Kim and T. Ura, "Fuel-optimally guided navigation and tracking control of auv under current interaction," in *Proceedings of the OCEANS'03, San Diego, California, USA*, 2003.

[3] L. Lapierre, D. Soetanto, and A. Pascoal, "Nonlinear path following with applications to the control of autonomous underwater vehicles," in *Proceedings of the 42nd IEEE CDC, Maui, Hawaii, USA*, 2003.

[4] A. J. Healey and D. Lienard, "Multivariable sliding-mode control for autonomous diving and steering of unmanned underwater vehicles," *IEEE Journal of Oceanic Engineering*, vol. 18, no. 3, pp. 327–339, 1993.

[5] P. Encarnação and A. Pascoal, "3D path following for autonomous underwater vehicle," in *Proceedings of the 39th IEEE CDC, Sydney, Australia*, 2000.

[6] K. D. Do and J. Pan, "Robust and adaptive path following for underactuated autonomous underwater vehicles," in *Proceedings of the ACC'03, Denver, Colorado, USA*, 2003.

[7] A. P. Aguiar and J. P. Hespanha, "Logic-based switching control for trajectory-tracking and path-following of underactuated autonomous vehicles with parametric modeling uncertainty," in *Proceedings of the ACC'04, Boston, Massachusetts, USA*, 2004.

[8] R. Skjetne, "The maneuvering problem," Ph.D. dissertation, Norwegian University of Science and Technology, Trondheim, Norway, 2005.

[9] M. Breivik and T. I. Fossen, "Principles of guidance-based path following in 2D and 3D," in *Proceedings of the 44th IEEE CDC, Seville, Spain*, 2005.

[10] F. A. Papoulias, "Bifurcation analysis of line of sight vehicle guidance using sliding modes," *International Journal of Bifurcation and Chaos*, vol. 1, no. 4, pp. 849–865, 1991.

[11] A. Teel, E. Panteley, and A. Loría, "Integral characterization of uniform asymptotic and exponential stability with applications," *Mathematics of Control, Signals, and Systems*, vol. 15, pp. 177–201, 2002.

[12] T. I. Fossen, *Marine Control Systems: Guidance, Navigation and Control of Ships, Rigs and Underwater Vehicles*, 1st ed. Marine Cybernetics, Trondheim, Norway, 2002.

[13] The Society of Naval Architects and Marine Engineers, "Nomenclature for treating the motion of a submerged body through a fluid," 1950, Technical and Research Bulletin No. 1-5.

[14] B. Stevens and F. Lewis, *Aircraft Control and Simulation*, 2nd ed. John Wiley & Sons Inc., 2003.

[15] T. I. Fossen, M. Breivik, and R. Skjetne, "Line-of-sight path following of underactuated marine craft," in *Proceedings of the 6th IFAC MCMC, Girona, Spain*, 2003.